

Radiative Physics in Charmonium from Lattice QCD

Jozef J. Dudek^{1,2}, Robert G. Edwards¹, Nilmani Mathur¹, David G. Richards¹

¹ Theory Center, Jefferson Laboratory MS12H2, 12000 Jefferson Avenue, Newport News, VA 23606, USA

² Department of Physics, Old Dominion University, 4600 Elkhorn Avenue, Norfolk, VA 23529, USA

E-mail: dudek@jlab.org

Abstract. Charmonium is an attractive system for the application of lattice QCD methods owing to the possibility of computing with the physical quark mass in a reasonable time. While the sub-threshold spectrum has been considered in some detail in previous works, it is only very recently that further properties such as radiative transitions and two-photon decays have come to be calculated; herein we discuss this recent progress.

1. Introduction

Between 3 and 3.7 GeV a number of states exist which are believed to be the bound states of a charm quark and an anti-charm quark and whose widths are narrow owing to their being below the threshold to decay to a pair of open charm mesons coupled with the suppression of annihilation channels at this high mass scale. Because the hadronic contributions to their widths are so small, radiative transitions between them constitute considerable branching fractions, and the rates of these transitions have been measured with some accuracy by a number of experiments [1]. Additionally the $C = +$ states can decay to a pair of photons - this process when time-reversed can serve as a production mechanism (two-photon fusion) at e^+e^- machines.

Rates for these radiative processes have been computed in various varieties of quark-model, and are typically fairly successful when one sets parameters using the experimental spectrum, however corrections beyond approximations like non-relativistic dynamics are often uncontrolled in these models.

In two recent papers, these quantities were addressed in a relativistic, field-theoretic realization of QCD. The theory is rendered computable by considering space-time to be a finite grid of points, allowing numerical evaluation of Euclidean correlation functions. Additionally, an approximation is made in that the effect of light-quark degrees-of-freedom were neglected, as were the effects of closed charm-quark loops. This 'quenched' approximation is a reasonable approximation to a version of QCD in which there is one heavy flavour of quark - its main differences with respect to the theory manifested in nature is believed to lie in the incorrect running of the coupling (via an incorrect beta-function) and the neglect of coupling to open charm meson decay channels.

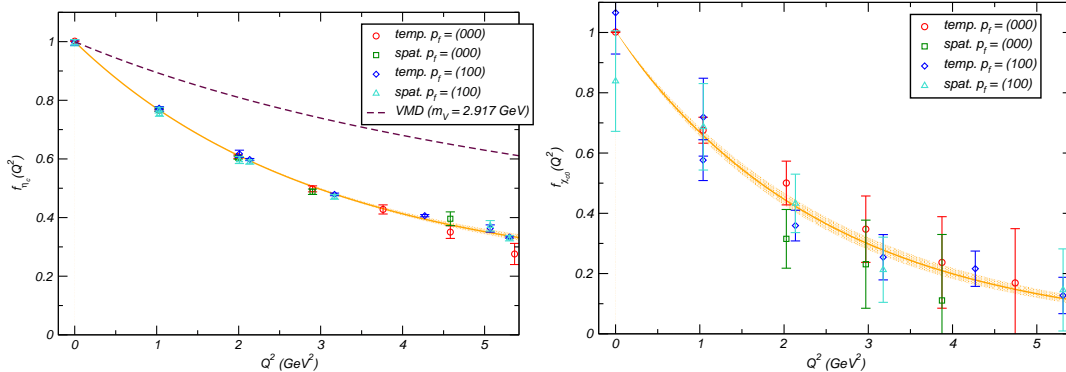


Figure 1. "form-factors" of (a) η_c and (b) χ_{c0}

2. Radiative Transitions

In [2], radiative transitions between charmonium states were extracted from a combination of two- and three-point functions. Details can be found in [2], here we will just mention that we used Domain Wall Fermions on anisotropic quenched lattices with antiperiodic boundary conditions in the temporal direction. We warn the reader that these are computations at one lattice spacing only, so that one should assume some undetermined systematic error from extrapolation to the continuum.

2.1. Vector Current "Form-Factors"

Charge-conjugation eigenstates do not have electromagnetic form-factors. At the quark level this can be attributed to the equal and opposite charge of the quark and the antiquark. Nevertheless by coupling a vector current to the quark only one can measure a "form-factor" that gives information about the internal structure of the state.

The η_c , analogously to the pion, has one vector form factor defined by $\langle \eta_c(\vec{p}') | j^\mu(0) | \eta_c(\vec{p}) \rangle = f_{\eta_c}(Q^2)(p' + p)^\mu$. Figure 1(a) shows $f_{\eta_c}(Q^2)$ as extracted in this calculation.

The orange curve in Figure 1 is the result of a fit to the data assuming the form $f(Q^2) = \exp[-\frac{Q^2}{16\beta^2}(1 + \alpha Q^2)]$ where $\beta = 480(3) \text{ MeV}$, $\alpha = -0.046(1) \text{ GeV}^{-2}$. This corresponds to a 'vector current radius' of 0.25 fm, somewhat justifying our use of a box of spatial length 1.2 fm. These numerical results are compared with quark models in [3].

The J/ψ , like the deuteron, has three vector current form-factors. A convenient set, known as the charge, magnetic dipole and electric quadrupole form-factors are defined in e.g. Ref [2]. Our results are shown in figure 2. Note that they are in accord with non-relativistic intuition - the charge radius is rather similar to that of the η_c , the magnetic dipole moment ($\mu = \frac{G_M(0)}{2M_{J/\psi}}$) is rather close to 2, and the quadrupole moment (corresponding to D -wave admixture) is very small.

The scalar χ_{c0} has a form-factor decomposition identical to the η_c . Our results, shown in figure 1(b) indicate a larger charge radius than the η_c as expected for a P -wave state with a centrifugal barrier.

2.2. Transition Form-Factors

Radiative transition rates with real ($Q^2 = 0$) transverse photons have been measured for a number of charmonium states. Our lattice kinematics are such that we can explore the transition form-factors as a function of Q^2 for both transverse and longitudinal photons. Our general method is to express the matrix element in terms of multipoles.

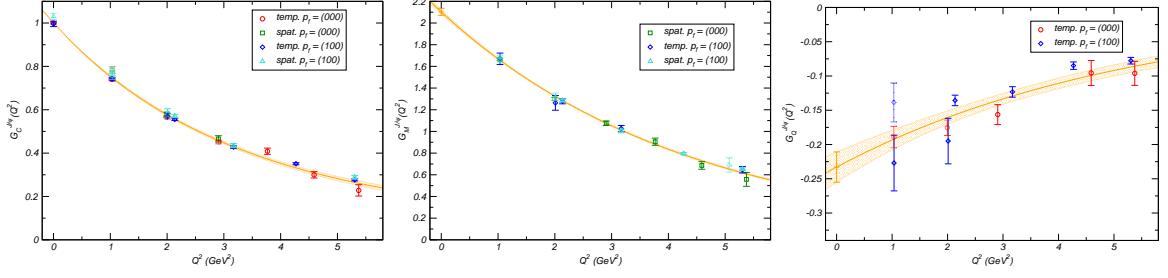


Figure 2. “form-factors” of the J/ψ

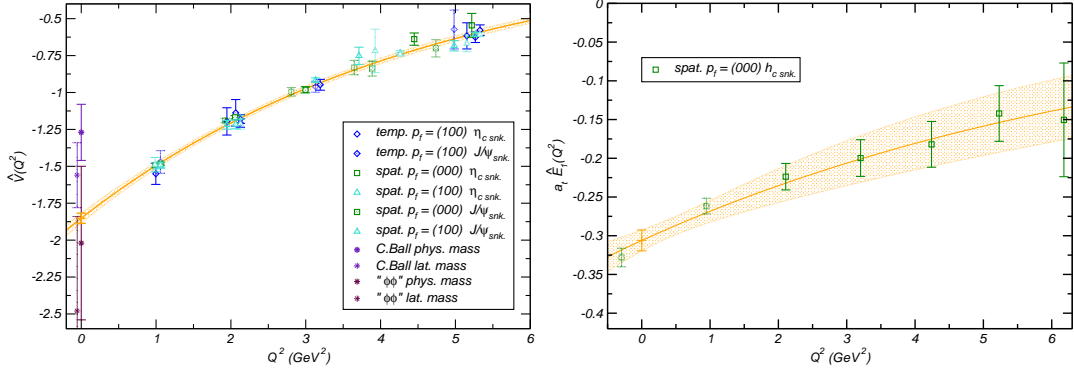


Figure 3. Transition form-factors for (a) $J/\psi \rightarrow \eta_c \gamma$ and (b) $h_c \rightarrow \eta_c \gamma$

The $J/\psi \rightarrow \eta_c$ transition has only a single, magnetic dipole ($M1$) contribution:

$$\langle \eta_c(\vec{p}') | j^\mu(0) | J/\psi(\vec{p}, r) \rangle = \frac{2V(Q^2)}{m_{\eta_c} + m_\psi} \epsilon^{\mu\alpha\beta\gamma} p'_\alpha p_\beta \epsilon_\gamma(\vec{p}, r). \quad (1)$$

In figure 3 we plot \hat{V} defined by $V(Q^2) = 2 \times \frac{2}{3} e \times \hat{V}(Q^2)$. The relation to the decay width is

$$\Gamma(J/\psi \rightarrow \eta_c \gamma) = \alpha \frac{|\vec{q}|^3}{(m_{\eta_c} + m_\psi)^2} \frac{64}{27} |\hat{V}(0)|^2. \quad (2)$$

The data is fitted with an exponential in Q^2 which allows the extrapolation back to the physical photopoint.

There is only one direct experimental measurement of this width [4], $\Gamma_{CB}(J/\psi \rightarrow \eta_c \gamma) = 1.14(33)\text{keV}$. Also shown is an indirect estimate constructed from product branching ratios.

There is an essential ambiguity in how we compare our lattice results with the experimental data which arises from the fact that our charmonia masses, as computed on this lattice, do not coincide exactly with the physical masses. The problem lies in whether we should use experimental or lattice masses in equation 2. $|\vec{q}|$ is closely related to the hyperfine splitting which is rather sensitive to details of the lattice calculation, hence we observe considerable difference in using lattice or experimental masses.

The $\chi_{c0} \rightarrow J/\psi \gamma$ transition has both a transverse, electric dipole form-factor (E_1) and a longitudinal form-factor C_1 . The covariant multipole decomposition is derived in [2] and shown

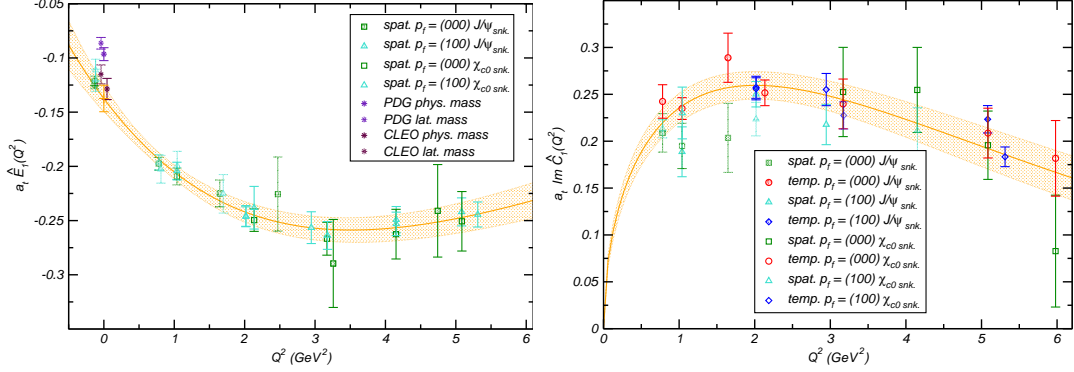


Figure 4. Transition form-factors for $\chi_{c0} \rightarrow J/\psi\gamma$. (a) E_1 multipole, (b) C_1 multipole

below

$$\langle \chi_{c0}(\vec{p}_S) | j^\mu(0) | J/\psi(\vec{p}_V, r) \rangle = \Omega^{-1}(Q^2) \left(E_1(Q^2) \left[\Omega(Q^2) \epsilon^\mu(\vec{p}_V, r) - \epsilon(\vec{p}_V, r) \cdot p_S (p_V^\mu p_V \cdot p_S - m_V^2 p_S^\mu) \right] + \frac{C_1(Q^2)}{\sqrt{q^2}} m_V \epsilon(\vec{p}_V, r) \cdot p_S \left[p_V \cdot p_S (p_V + p_S)^\mu - m_S^2 p_V^\mu - m_V^2 p_S^\mu \right] \right).$$

At the photopoint there are no longitudinal photons and the width is given by

$$\Gamma(\chi_{c0} \rightarrow J/\psi\gamma) = \alpha \frac{|\vec{q}|}{m_{\chi_{c0}}^2} \frac{16}{9} |\hat{E}_1(0)|^2. \quad (3)$$

Our results are shown in figure 4. The fit form for $E_1(Q^2)$ is

$$\hat{E}_1(Q^2) = \hat{E}_1(0) \left(1 + \frac{Q^2}{\rho^2} \right) \exp \left[-\frac{Q^2}{16\beta^2} \right], \quad (4)$$

which will be discussed later in the context of the non-relativistic quark model. The fit is excellent and notably extrapolates through the negative Q^2 points which were not included in the fit. The agreement with PDG and CLEO data at $Q^2 = 0$ is quite encouraging.

With real photons the $\chi_{c1} \rightarrow J/\psi$ transition receives contributions from two multipoles, the dominant electric dipole (E_1) and a much suppressed magnetic quadrupole (M_2). Experimentally the M_2 contribution is measured through the angular distribution of photons - the PDG[1] average the two extractions performed[5, 6], each of which found a number consistent with zero, to give

$$\frac{M_2(0)}{\sqrt{E_1(0)^2 + M_2(0)^2}} = -0.002_{-0.017}^{+0.008}. \quad (5)$$

The covariant relation connecting the transition matrix element with the multipole amplitudes is given in [2]. Results are shown in figure 5, where agreement with experiment within large lattice statistical error bars is seen.

The h_c , with $J^{PC} = 1^{+-}$, was only recently observed with high significance by the CLEO collaboration [8, 7]. The reason for the delay of discovery with respect to the other ground

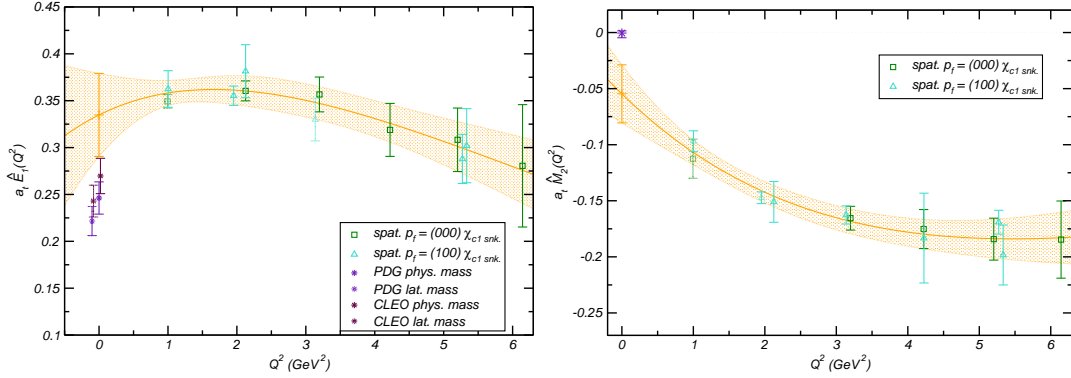


Figure 5. Transition form-factors for $\chi_{c1} \rightarrow J/\psi\gamma$. (a) E_1 multipole, (b) M_2 multipole.

state charmonia lies in the difficulty of production - the process eventually utilised was the isospin violating $\psi(2S) \rightarrow \pi^0 h_c$ with a subsequent $h_c \rightarrow \eta_c \gamma$. Since only the product branching fraction $\mathcal{B}(\psi(2S) \rightarrow \pi^0 h_c) \mathcal{B}(h_c \rightarrow \eta_c \gamma)$ is measured, our calculation of $\Gamma(h_c \rightarrow \eta_c \gamma)$ constitutes a prediction.

The form-factor decomposition is identical to the $\chi_{c0} \rightarrow J/\psi\gamma$ case. We plot the extracted $E_1(Q^2)$ in figure 3(b).

Our value at $Q^2 = 0$ corresponds to a width

$$\Gamma(h_c \rightarrow \eta_c \gamma) = \frac{663(132)}{601(55)} \text{ keV}. \quad (6)$$

where the upper value uses lattice masses and the lower value physical masses with the difference indicative of lattice systematic errors.

The fit forms we have used are motivated by the kind of functional forms one gets in simple non-relativistic quark models and indeed the β and ρ values we extract are very much in line with the expectations of such models, see [2] for details.

3. Two-Photon Decays

At first sight it is not clear how one would go about evaluating the matrix element for the process $\eta_c \rightarrow \gamma\gamma$ in lattice QCD. In the previous section we outlined how to extract the matrix element for a radiative transition between two QCD eigenstates from a three-point function evaluated at large Euclidean times. This issue here is that the photon is not an eigenstate of QCD - taking a vector interpolating field to large Euclidean time would not yield a photon state, but instead the lightest QCD vector eigenstate (the J/ψ in this case).

However, all is not lost, for while the photon is not a QCD eigenstate, it can be constructed from a linear superposition of QCD eigenstates. The precise field-theoretic mechanism for this is the LSZ reduction. The connection in Euclidean space-time, for a different physical process, is made in [9] and for the process in question an outline appears in [10]. The end result is that the following equation connects the matrix element of interest to a Euclidean three-point function computable on the lattice: $\langle M(p) | \gamma(q_1, \lambda_1) \gamma(q_2, \lambda_2) \rangle = \lim_{t_f \rightarrow \infty}$

$$e^2 \frac{\epsilon_\mu(q_1, \lambda_1) \epsilon_\nu(q_2, \lambda_2)}{2E_M(p)} e^{-E_M(p)(t_f-t)} \int dt_i e^{-\omega_1(t_i-t)} \langle 0 | T \left\{ \int d^3 \vec{x} e^{-i\vec{p}\cdot\vec{x}} \varphi_M(\vec{x}, t_f) \int d^3 \vec{y} e^{i\vec{q}_2\cdot\vec{y}} j^\nu(\vec{y}, t) j^\mu(\vec{0}, t_i) \right\} | 0 \rangle \quad (7)$$

The difference with respect to the radiative transitions between hadrons considered above is that an integral over the Euclidean time position of a vector source is now involved.

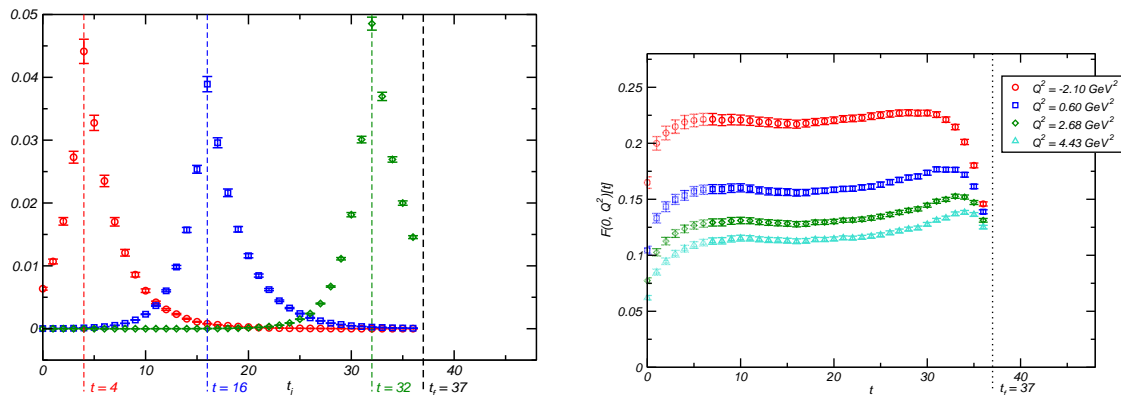


Figure 6. (a) Integrand in equation 7 at three values of vector current insertion time ($t = 4, 16, 32$) with pseudoscalar sequential source at sink position $t_f = 37$. (b) Pseudoscalar two-photon form-factor as a function of time slice, t , from equation 7. First six time slices ghosted out due to the Dirichlet wall truncating the integral.

In this case an isotropic $24^3 \times 48$ lattice with $a = 0.047 \text{ fm}$ [11] was utilised, with a non-perturbatively determined Clover fermion action[12] and Dirichlet temporal boundary conditions. While the computation cost was reduced with respect to the DWF used previously, we had to accept the possibility of larger discretisation errors. We used the conserved vector current[13].

In figure 6(a) we display the integrand of equation 7, having computed with a pseudoscalar interpolating field fixed at $t = 37$, a conserved vector current insertion at $t = 4, 16, 32$ and a vector interpolating field at all possible source positions, $t = 0 \rightarrow 37$. It is clear that provided one is not too close to the Dirichlet wall or to the sink position, one can capture the entire integral by summing timeslices. In figure 6(b) the results of summing timeslices to compute the integral for all possible insertion positions and a number of Q^2 are shown.

Given the confidence that the integral can be captured on a lattice of this temporal length, one can use a much faster method to compute the transition form-factor that places the sum over timeslices into a 'sequential source', reducing the computation time by a factor of $\mathcal{O}(L_t)$.

The Clover fermion action is 'improved' in that it seeks to reduce the effect of $\mathcal{O}(a)$ discretisation errors on extracted quantities (relative to the Wilson fermion action). The same improvement procedure that is applied to the action can be applied to the operators that appear in matrix-elements. Since the publication of [10] we have reanalysed our data implementing the conserved, improved vector current of [13]. The results, for the faster 'photon as sequential source' method, are shown in figure 7 along with the results using just a conserved current. The difference indicates the degree to which $\mathcal{O}(a)$ discretisation errors may be affecting our results - future computations will need to consider the a -scaling behaviour of these quantities.

The $\eta_c \rightarrow \gamma\gamma^*$ data is fitted with a simple one pole parameterisation $F(Q^2) = F(0)/(1 + \frac{Q^2}{\mu^2})$. The result $F(0) = 0.210(5)$ (where the error is purely statistical, taking no account of the discretisation or quenching uncertainties) is in approximate agreement with the experimental value. The effective pole position $\mu = 3.43(3) \text{ GeV}$ is somewhat larger than the J/ψ mass indicating that in a vector meson dominance approach one would need to consider the effect of excited vector charmonia. More precise data might allow a fit more sophisticated than this simple one-pole form.

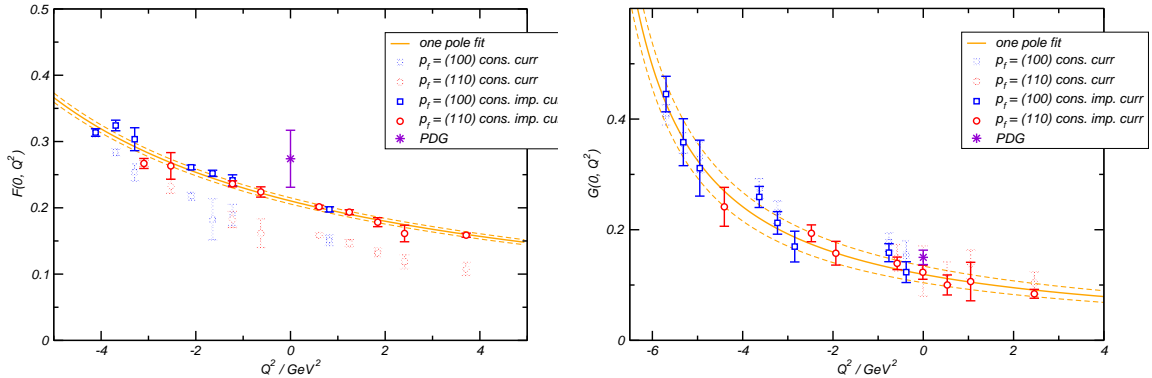


Figure 7. (a) $\eta_c \rightarrow \gamma\gamma^*$ amplitude. (b) $\chi_{c0} \rightarrow \gamma\gamma^*$ amplitude. Fits are one-pole forms as described in the text. Solid points use the conserved improved current while the ghosted points use only the conserved current.

The $\chi_{c0} \rightarrow \gamma\gamma^*$ data fit yields $G(0) = 0.119(15)$ and $\mu = 2.81(4)$ GeV.

4. Higher Spins, Exotic J^{PC} and Excited States

In [2, 10] only states with $J^{PC} = 0^{\pm+}, 1^{--}, 1^{+\pm}$ were considered. This limitation arises from the choice of $\bar{\psi}(x)\Gamma\psi(x)$ as meson interpolating field. States of other J^{PC} can be accessed by introducing covariant derivatives into the fermion bilinear, e.g. $\bar{\psi}\Gamma(\overrightarrow{D}_j - \overleftarrow{D}_j)\psi$ [14]. By using the symmetrised derivative one ensures eigenstates of charge conjugation at finite three-momentum.

We show in figure 8 some preliminary effective mass plots using operators of this type.

As well as higher spins we are also interested in excited states within a given J^{PC} . Extracting excited state transitions from Euclidean three-point functions is a challenging task since it requires one to accurately consider the sub-leading exponentials. In principle if one has accurately extracted masses and overlap factors for the excited states from two-point functions one can fit for the excited state transitions simultaneously with the ground state transition. In [2] this was found to be unsuccessful owing to an unfortunate side-effect of using temporal anti-periodicity where other time-orderings mimicked excited states.

Currently work using dirichlet temporal boundary conditions seems to indicate that given sufficiently precise two-point function fits, one can extract excited state transitions, although with very much larger statistical errors than in the case of ground-state transitions.

5. Summary

First investigations of radiative transitions using lattice QCD have been performed and the results are promising given caveats surrounding the quenched approximation and computation at a single lattice spacing. With the three-point function technology now developed, future studies can endeavour to get control of the systematic errors by moving to dynamical gauge fields and computing at multiple lattice spacings.

Notice: Authored by Jefferson Science Associates, LLC under U.S. DOE Contract No. DE-AC05-06OR23177. The U.S. Government retains a non-exclusive, paid-up, irrevocable, worldwide license to publish or reproduce this manuscript for U.S. Government purposes.

References

- [1] W. M. Yao *et al.* [Particle Data Group], J. Phys. G **33** (2006) 1.
- [2] J. J. Dudek, R. G. Edwards and D. G. Richards, Phys. Rev. D **73**, 074507 (2006) [arXiv:hep-ph/0601137].
- [3] O. Lakhina and E. S. Swanson, Phys. Rev. D **74** (2006) 014012 [arXiv:hep-ph/0603164].

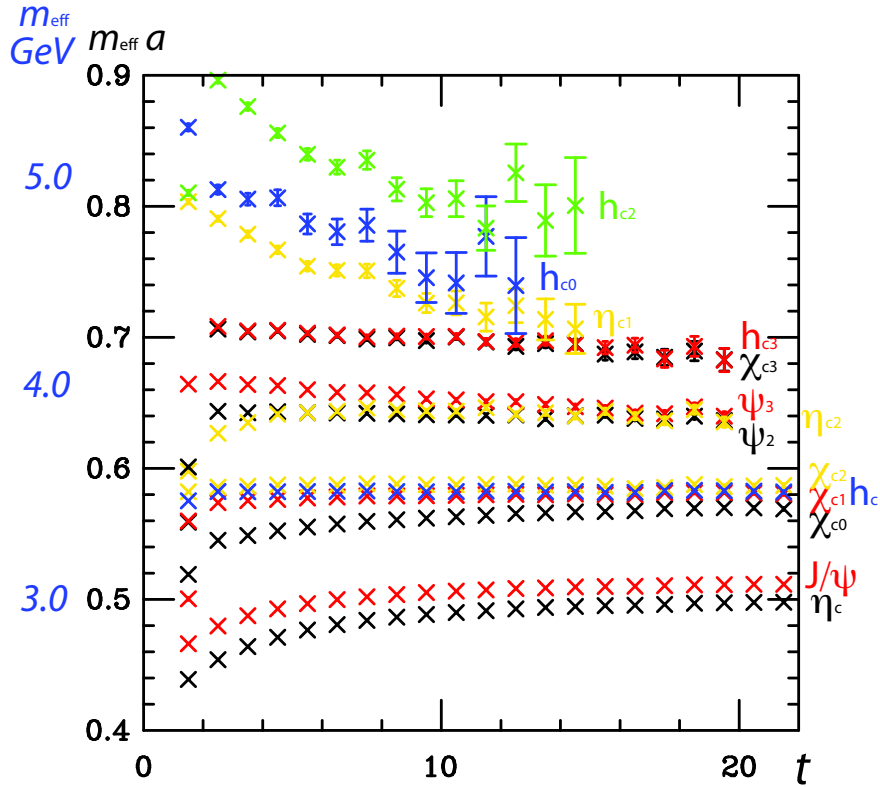


Figure 8. Preliminary charmonium effective masses using derivative-based interpolating fields. Note that the heaviest three quantum numbers are exotic.

- [4] J. Gaiser *et al.*, Phys. Rev. D **34** (1986) 711.
- [5] M. Ambrogiani *et al.* [E835 Collaboration], “Study of the angular distributions of the reactions anti-p p \rightarrow χ /c1, Phys. Rev. D **65**, 052002 (2002).
- [6] M. Oreglia *et al.*, Phys. Rev. D **25**, 2259 (1982).
- [7] P. Rubin *et al.* [CLEO Collaboration], Phys. Rev. D **72**, 092004 (2005) [arXiv:hep-ex/0508037].
- [8] J. L. Rosner *et al.* [CLEO Collaboration], Phys. Rev. Lett. **95**, 102003 (2005) [arXiv:hep-ex/0505073].
- [9] X. d. Ji and C. w. Jung, Phys. Rev. Lett. **86**, 208 (2001) [arXiv:hep-lat/0101014].
- [10] J. J. Dudek and R. G. Edwards, Phys. Rev. Lett. **97**, 172001 (2006) [arXiv:hep-ph/0607140].
- [11] R. G. Edwards, U. M. Heller and T. R. Klassen, Nucl. Phys. B **517**, 377 (1998) [arXiv:hep-lat/9711003].
- [12] M. Luscher, S. Sint, R. Sommer, P. Weisz and U. Wolff, Nucl. Phys. B **491**, 323 (1997) [arXiv:hep-lat/9609035].
- [13] G. Martinelli, C. T. Sachrajda and A. Vladikas, Nucl. Phys. B **358** (1991) 212.
- [14] X. Liao and T. Manke, arXiv:hep-lat/0210030.